AIMS Mathematics, 7(12): 20594–20614.
DOI:10.3934/math.20221129
Received: 28 July 2022
Revised: 04 September 2022
Accepted: 13 September 2022
Published: 21 September 2022

http://www.aimspress.com/journal/Math

Research article

Differential order analysis and sensitivity analysis of a CoVID-19 infection system with memory effect

Mohammad Sajid[1,*], **Biplab Dhar**[2] **and Ahmed S. Almohaimeed**[3]

[1] Department of Mechanical Engineering, College of Engineering, Qassim University, Buraydah 51452, Saudi Arabia
[2] Department of Mathematics-SoPS, DIT University, Dehradun 248009, Uttarakhand, India
[3] Department of Mathematics, College of Science, Qassim University, Buraydah 51452, Saudi Arabia

* **Correspondence:** Email: msajd@qu.edu.sa; Tel: +966163013761.

Abstract: The paper deals with numerical analysis of solutions for state variables of a CoVID-19 model in integer and fractional order. The solution analysis for the fractional order model is done by the new generalized Caputo-type fractional derivative and Predictor-Corrector methodology, and that for the integer order model is carried out by Multi-step Differential Transformation Method. We have performed sensitivity analysis of the basic reproduction number with the help of a normalized forward sensitivity index. The Arzelá-Ascoli theorem and Fixed point theorems with other important properties are used to establish a mathematical analysis of the existence and uniqueness criteria for the solution of the fractional order. The obtained outcomes are depicted with the help of diagrams, narrating the nature of the state variables. According to the results, the Predictor-Corrector methodology is favorably unequivocal for the fractional model and very simple in administration for the system of equations that are non-linear. The research done in this manuscript can assure the execution and relevance of the new generalized Caputo-type fractional operator for mathematical physics.

Keywords: Chebyshev norms; trapezoidal quadrature rule; Adams-Bashforth method; memory effect; Ms-DTM; Caputo-type fractional derivative
Mathematics Subject Classification: 26A33, 92-10, 92D25

1. Introduction

We, here, present a brief introduction, features, symptoms, etc. of the CoVID-19 pandemic; and methodologies for solving proposed systems of differential equations. The section will also have some recent motivating works from the field. The objectives of the article are also presented here. Mathematical forecasts in modeling the CoVID-19 pandemic are still in the pursue for its improvement.

The meteoric spread, the course of actions and the methods concerned in the containment of this disease demand the soonest and quickest understanding in perceiving solutions as in biological, environmental, and continual aspects of life with much better cognitive knowing by mathematical computerized modeling.

However, the effects on post-spread CoVID-19 infectiousness and evolution in contacted persons are not known fully. The signs and symptoms of all patients of CoVID-19 are more or less the same; they endure respiratory problems, fever, dry cough and so on with much more adverse conditions. Almost all countries are still suffering from the infection, and its destructiveness is ascending gradually. The disease is spreading among different countries, primarily via air travel [6], and the present occurrence are possibly because of our ignorance or casual thinking and way of living [4]. As a matter of fact, there are many looming queries about CoVID-19 spread, such as "number of individual that will be infected in the coming days," "timing of epidemic turning point," "infection during the peak and number of individuals that are infected at that time," and so on. Usually, in analysis of epidemiology, virus causal infections grow exponentially, maintaining a determined rate of reproduction [17]. We have considered the idea and presented a mathematical analysis of a CoVID-19 pandemiology. Systems comprising non-linear equations are beneficial for studying the complicated dynamical behaviour. The fractional calculus theory is very old and is presently a prime process to fulfill the needs in the study and analysis of physical world problems.

In this article, the results of the CoVID-19 infection model are analyzed with the help of a newly generalized Caputo-type fractional derivative (NGCFD) that shares the same salient features of the Caputo fractional derivative [22]. Presently, mathematical pandemiology is done with the help of fractional order derivatives by several researchers which can be found in the above cited articles. The Caputo derivative is appropriate for initial value problems (IVPs) and has many features that are similar to integer order derivatives [11]. The properties of the NGCFD and the Caputo derivative are precisely the same. The Predictor-Corrector (PC) scheme is one of the most well ordered, steady and error-free to evaluate infection IVPs, and therefore the scheme is used here. In the sense of the new generalized Caputo-type operator, the adaptive PC scheme uses a non-uniform mesh that varies with the PC scheme of Caputo operator. The NGCFD operator is highly impacted by the values of the parameters ξ and τ. Hence, it provides an important tool to authorize and develop mathematical fractional models which can be applied for physical world problems. These two parameters are important for sketching the true data during numerical and graphical simulations, and therefore this fractional derivative has some extra characteristics in comparison to non-singular kernel fractional derivatives.

An extensive mathematical study of the CoVID-19 model is made with consideration of both asymptomatic and symptomatic infected individuals by the ABC approach and the Caputo-based fractional compartmental model [1–3,10,20]. More than 80% of people who test positive for CoVID 19 do not show any symptoms of the infection for a long period [19]. This may have various reasons, such as age, gender, cross immunity, environment, etc. Nevertheless, it cannot be ignored that asymptomatic transmission is increasing the number of cases suffering from the disease. Thus, there is a dependency term of asymptomatic transmission to symptomatic transmission in CoVID-19 cases. This calls for hysteresis [7], commonly known as a memory effect, in pandemiology in the same way it is seen in epidemiology [5]. Mathematically, let $g(x_0, t)$ be a solution of a first order differential equation which is autonomous, having initial condition $x(t = 0) = x_0$. Now, it can be deduced that $g(x_0, t + \tau) = g(g(x_0, \tau), t)$. This implies that the solution remains invariant by taking initial conditions

as $g(x_0, \tau)$ because the term $g(x_0, \tau)$ lies in the solution space. Collectively, under a certain initial condition and for any point of region the solution is unique. However, if the order of the autonomous differential equation is a pure fraction, then introduction of a memory effect becomes essential. The memory effect is an important element in several biological phenomena and has been used frequently in various bio-mathematical models [5, 28]. Hence, it is practicable to use fractional alternatives, as fractional derivatives essentially involve the effect of memory. The study of the CoVID-19 infection real data for various regions is non-uniform with respect to time, and therefore, it is tedious to analyze the nature of state variables of the CoVID-19 infection model more precisely by integral derivative operators. There also lies ample scope of using fractional derivatives to do the mathematical study elaborately. In the year 2020, a comparison study was done on measles epidemics, and, depending on the data set, it was found that the fractional order system converged to the integer order system for a particular data set [12]. Similarly, many epidemics have been studied in terms of fractional and integer order models [15, 16, 21], and the concluding remarks are almost all in favour of the fractional order models. The question is whether, *in vivo* and/or *in vitro*, the merits of using fractional operators over ordinary operators supersede the added computational complexity.

Very recently, we have discussed how vaccination can lower the effects of infection during the pre-infection stage [9]. The numerical findings are supported by the Caputo-Fabrizio and the Caputo-sense Atangana-Baleanu non-singular kernel fractional derivative operators with memory effects. An individual cannot be exposed to the infection with a notion that vaccines are readily, and easily available. Also, it is a tedious task to identify the asymptomatic population irrespective of the economical structure of a society. This implies to include a model parameter that can relate the rate at which asymptomatic individuals show infection, that is, become a symptomatic, which is one of the aims of this article. The main goal is to study mathematically a fractional CoVID-19 infection model by the NGCFD with a PC scheme and then to compare the dynamical behaviour of state variables of the integer order CoVID-19 infection model by the Multi-step Differential Transformation Method (Ms-DTM). One of the merits of the Ms-DTM is that the series solution converges for broad time domains and can provide precise solutions for chaotic as well as non-chaotic systems [23]. The infection model is to be studied at various nearby fractional order values τ with the usage of an additional parameter ξ.

In Section 2, we recapitulate a few noteworthy results about the generalized fractional derivatives within the fractional calculus literature. Section 3 is about the description of the ordinary differential equation model, followed by the fractional order model. The basic mathematical analysis, such as existence, uniqueness, positivity and boundedness of solutions of the infection model, are done in Sections 4 and 5. Expression of the basic reproduction number with its biological interpretation is given in Section 6. Evaluation of the sensitivity index of the basic reproduction number with respect to some vital parameters involved in the system is presented in Section 7. The numerical simulations of both systems are put forward in Section 8, together with brief narration of the Ms-DTM and PC schemes, as well as the results obtained. At last, in Section 9, the article ends with the conclusions of the findings.

2. Recapitulation

Before pondering the complex dynamics of the infection model, let us get acquainted with the preliminary definitions, notations, and results about some popular fractional derivatives and the

NGCFD.

Definition 1. *[25] The non-integral Caputo order derivative of $f \in C_{-1}^{\kappa}$ is given by*

$$\mathcal{D}_t^{\tau} f(t) = \begin{cases} \dfrac{d^{\kappa}}{dt^{\kappa}} f(t), & \tau = \kappa \in \mathbb{N}, \\ \dfrac{1}{\Gamma(\kappa - \tau)} \displaystyle\int_0^t (t-v)^{\kappa-\tau-1} f^{(\kappa)}(v) dv, & \kappa - 1 < \tau < \kappa \in \mathbb{N}. \end{cases} \tag{2.1}$$

Definition 2. *[14] The generalized Riemann-type fractional derivative operator, ${}^{\mathcal{R}}\mathcal{D}_{b_+}^{\tau,\xi}$, of order $\tau > 0$ is given by:*

$$\left({}^{\mathcal{R}}\mathcal{D}_{b_+}^{\tau,\xi} f\right)(s) = \frac{\xi^{\tau-\kappa+1}}{\Gamma(\kappa-\tau)} \left(s^{1-\xi}\frac{d}{ds}\right)^{\kappa} \int_0^s y^{s-1} \left(s^{\xi} - y^{\xi}\right)^{\kappa-\tau-1} f(y) dy, \quad s > b, \tag{2.2}$$

where $\xi > 0$, $b \geq 0$, and $\kappa - 1 < \tau \leq \kappa$.

Definition 3. *[14] The generalized Caputo-type fractional derivative operator, ${}^{\mathcal{C}}\mathcal{D}_{b_+}^{\tau,\xi}$, of order $\tau > 0$ is given by:*

$$\left({}^{\mathcal{C}}\mathcal{D}_{b_+}^{\tau,\xi} f\right)(s) = \left({}^{\mathcal{R}}\mathcal{D}_{b_+}^{\tau,\xi}\left[f(y) - \sum_{u=0}^{\kappa-1} \frac{f^{(u)}(b)}{u!}(y-b)^u\right]\right)(s), \quad s > b, \tag{2.3}$$

where $\xi > 0$, $b \geq 0$, $\kappa = \lceil \tau \rceil$.

Definition 4. *[22] The NGCFD operator, ${}^{\mathcal{GC}}\mathcal{D}_{b_+}^{\tau,\xi}$, of order $\tau > 0$ is given by:*

$$\left({}^{\mathcal{GC}}\mathcal{D}_{b_+}^{\tau,\xi} f\right)(s) = \frac{\xi^{\tau-\kappa+1}}{\Gamma(\kappa-\tau)} \int_b^s y^{\xi-1} \left(s^{\xi} - y^{\xi}\right)^{\kappa-\tau-1} \left(y^{1-\xi}\frac{d}{dy}\right)^{\kappa} f(s) ds, \quad s > b, \tag{2.4}$$

where $\xi > 0$, $b \geq 0$, and $\kappa - 1 < \tau \leq \kappa$.

Lemma 1. *[18] If $\alpha \in \,]0,1[$, and $n \in \mathbb{N} \cup \{0\}$, then there exists constants $\mathfrak{C}_{\alpha,1}, \mathfrak{C}_{\alpha,2} \in \mathbb{N}$, dependent on α, such that*

$$(n+1)^{\alpha} - n^{\alpha} \leq \mathfrak{C}_{\alpha,1} (n+1)^{\alpha-1}$$

and

$$(n+2)^{\alpha+1} - 2(n+1)^{\alpha+1} + n^{\alpha+1} \leq \mathfrak{C}_{\alpha,2} (n+1)^{\alpha-1}.$$

Lemma 2. *[18] Let us say that $\delta_{\rho,n} = (n-\rho)^{\alpha-1}$, where $\rho = 1, 2, 3, \cdots, (n-1)$, and $\delta_{\rho,n} = 0$ for $\rho = n, \alpha, \mathcal{M}, h, \mathcal{T} > 0$, $mh \leq \mathcal{T}$ and $m \in \mathbb{N}$. Let, $\displaystyle\sum_{\rho=m}^{n} \delta_{\rho,n}|e_{\rho}| = 0$ for $n \in [1, \kappa[$.*

If $|e_n| \leq \mathcal{M}h^{\alpha} \displaystyle\sum_{\rho=1}^{n-1} \delta_{\rho,n}|e_{\rho}| + |\eta|$, $n = 1, 2, 3, \cdots, m$ then $|e_m| \leq \mathfrak{C}|\eta|$, $m = 1, 2, \cdots$, where $\mathfrak{C}$ is a positive constant not dependent on m and h.

3. The proposed CoVID-19 infection model

A social system faces and experiences several challenges or problems in tackling an emergency; therefore, a proper mathematical model is of great significance for analyzing the impacts of sudden protocols on populaces. The importance of having an efficient source of applicable information or data that gives leaders quick, simple and productive solutions that fit best is important in implementing and strategy objectives.

In this paper, CoVID-19 infection spread is taken as human to human and is a four compartments model with populaces of Susceptibles, $S(t)$; Asymptomatic infectious people, $A(t)$; and Infected with symptoms, $I(t)$, called Symptomatics, at any time t. An SEIR CoVID-19 model [24] allows us to calculate the number of infections considering the chaotic contributions of the model's state variables. The model in this article is a modified model where the rate at which the susceptible populaces are born and the natural death rate of all the state variables are taken into consideration, and it is completely focused on the relationship between $A(t)$ and $I(t)$. So, in the sense of ordinary derivatives, the integer order model is

$$\begin{aligned} \frac{d}{dt}S(t) &= \lambda - \beta S\,(A + I) - dS, \\ \frac{d}{dt}A(t) &= \beta S\,(A + I) - \eta A - dA, \\ \frac{d}{dt}I(t) &= \eta A - \mu I - dI, \end{aligned} \tag{3.1}$$

with initial conditions $S(0) = S_0 > 0$, $A(0) = A_0 > 0$, $I(0) = I_0 > 0$. The Figure 1 depicts the relationship amongst state variables including all parameters. The parameters involved in the system (3.1) are described as follows:

i) λ : natural human birth rate,
ii) β : the rate at which the infection is spreading between susceptible and asymptomatic infectious individuals,
iii) d : natural death rate of state variables,
iv) η : the rate at which the infection is spreading between symptomatics and asymptomatics,
v) μ : rate at which infected with symptoms die due to severe infection.

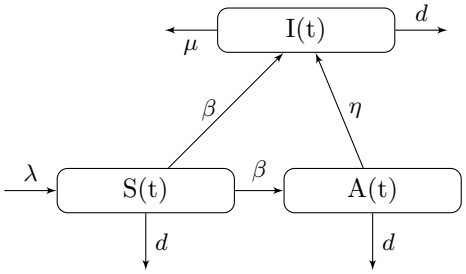

Figure 1. Box diagram representing relation of state variables and parameters involved in the CoVID-19 infection model.

The rate λ is considered to be unity, which means that every single individual is vulnerable to the infection. A few biological parameters are adjusted to assure that both sides of the model (3.1) have the same dimension $(time)^{\tau}$ [13]. Now, the proposed system (3.1) in the NGCFD with memory effect, τ, is as follows:

$$\begin{aligned}
\left({}^{C}\mathcal{D}_{t}^{\tau,\xi}\right) S(t) &= \lambda^{\tau} - \beta^{\tau} S\,(A+I) - d^{\tau} S,\\
\left({}^{C}\mathcal{D}_{t}^{\tau,\xi}\right) A(t) &= \beta^{\tau} S\,(A+I) - \eta^{\tau} A - d^{\tau} A,\\
\left({}^{C}\mathcal{D}_{t}^{\tau,\xi}\right) I(t) &= \eta^{\tau} A - \mu^{\tau} I - d^{\tau} I.
\end{aligned} \tag{3.2}$$

Now, for simplicity, the system (3.2) in compact form can be written as follows:

$$\begin{aligned}
\left({}^{C}\mathcal{D}_{t}^{\tau,\xi}\right) S(t) &= \mathcal{G}_1(S,t),\\
\left({}^{C}\mathcal{D}_{t}^{\tau,\xi}\right) A(t) &= \mathcal{G}_2(A,t),\\
\left({}^{C}\mathcal{D}_{t}^{\tau,\xi}\right) I(t) &= \mathcal{G}_3(I,t),
\end{aligned} \tag{3.3}$$

with the same initial conditions as given for system (3.1).

Table 1. The baseline values of the parameters and that of τ are estimated and taken from Dhar *et al*. [9] and Erturk *et al*. [10].

τ	β	μ	d	λ	η
1, 0.98, 0.95, 0.92	4.44×10^{-8}	$\frac{1}{7}$	0.01	1	0.14285

4. Basic properties of system (3.1)

Here, we discuss the existence, positivity, and boundedness of the solutions of the system, by providing necessary theorems [8], under the initial conditions. Before we proceed, it is necessary to provide a justification that the value of every state variable is positive for all $t \geq 0$.

4.1. Existence and positivity of solutions

For the sake of simplicity, let us consider that the sum of all the state variables is $\mathfrak{N}(t)$. Therefore,

$$\frac{d}{dt}\mathfrak{N}(t) \;=\; \lambda - d\mathfrak{N} - \mu I. \tag{4.1}$$

Solving Eq (4.1), we get, $\limsup_{t\to\infty} \mathfrak{N}(t) \leq \dfrac{\lambda}{d}$. Therefore, the system is feasible in the region $\mathcal{W} = \left\{(S,A,I) \in \mathbb{R}_3^+ : 0 < \mathfrak{N} \leq \dfrac{\lambda}{d}\right\}$.

The set $\mathcal{W}$ is now a positive invariant set, which means that the system is pandemiologically well-ordered, and the solutions of the system remains in $\mathcal{W}$.

Theorem 1. *The solutions of the IVP (3.1) are positive for all $t \geq 0$.*

Proof. We apply the method of variation of constants for the system under the initial conditions. From the first equation of the system, we have

$$\frac{d}{dt}S(t) + \{\beta(A(t) + I(t)) + d\}S(t) = \lambda.$$

Therefore,

$$S(t) = \left\{S_0 + \lambda \int_0^t e^{\int_0^s \{\beta(A(x) + I(x)) + d\}dx} ds\right\} \times e^{\int_0^t -\{\beta(A(x) + I(x)) + d\}dx}.$$

Similarly, from the other two equations of the system (3.1), we have, respectively,

$$A(t) = \left\{A_0 + \beta \int_0^t S(s)I(s)e^{\int_0^s \{\eta + d - \beta S(x)\}dx} ds\right\} \times e^{\int_0^t \{-\eta - d + \beta S(x)\}dx},$$

$$I(t) = \left\{I_0 + \eta \int_0^t A(s)e^{(\mu+d)s} ds\right\} \times e^{-(\mu+d)t}.$$

Clearly, with regard to the initial conditions, it can be deduced that $S(t) > 0$, $A(t) > 0$, and $I(t) > 0$. This implies that the solution of IVP (3.1) with the initial conditions exists and is unique on $\mathcal{W}$ for all $t \geq 0$, because the right-hand side of the system is local Lipschitzian [8] and completely continuous on the space of continuous functions. □

4.2. Boundedness of solutions

Theorem 2. *With positive initial conditions, the solutions of the IVP (3.1) are bounded.*

Proof. Let us consider any positive solution $(S, A, I) \in \mathcal{W}$ of the system. We construct a Lyapunov function $L_f(t) = S + A + I$. Differentiating L_f w.r.t. t along the system, we get

$$\begin{aligned}\frac{dL_f}{dt} &= \lambda - d\mathfrak{N} - \mu I \\ &= \lambda - (d\mathfrak{N} + \mu I).\end{aligned}$$

We now see that $\frac{dL_f}{dt} > 0$ or < 0, accordingly, if $\lambda > d\mathfrak{N} + \mu I$ or $\lambda < d\mathfrak{N} + \mu I$, respectively. This implies that any solution starting from a positive initial value must be bounded [8]. The boundedness of a solution also shows that it exists for all $t \geq 0$, by the continuation theory of ordinary differential equations. Therefore, the solutions of the IVP (3.1) are bounded. □

5. Basic properties of system (3.2)

The existence of a unique solution, and positivity of the proposed model (3.2) are given by the consequences of fixed point theory. The analysis for susceptible populaces is focused on, and the rest

of the state variables will be done in a similar manner. We consider the IVP (first equation of the system (3.2))

$$\begin{aligned} \left({}^{C}\mathcal{D}_{t}^{\tau,\xi}\right) S(t) &= \mathcal{G}_1(S,t), \\ S(0) &= S_0. \end{aligned} \tag{5.1}$$

The corresponding solution for Eq (5.1) is a Volterra integral equation, given by

$$S(t) \;=\; S_0 + \frac{\xi^{1-\tau}}{\Gamma(\tau)} \int_0^t z^{\xi-1} \left(t^{\xi} - z^{\xi}\right)^{\tau-1} \mathcal{G}_1(S,z)\, dz. \tag{5.2}$$

5.1. Existence and positivity of solution

The following results are presented in the forms of a theorem and a lemma for showing the existence of a solution.

Theorem 3. *Let* $0 < \tau \leq 1$, $S_0 \in \mathbb{R}$, $L > 0$ *and* $\mathbb{A}^* > 0$. *Define* $\Omega := \{(t,S) : t \in [0,\mathbb{A}^*], |S - S_0| \leq L\}$, *and let the function* $\mathcal{G}_1 : \Omega \to \mathbb{R}$ *be continuous. Further, define* $U := \sup_{(t,S)\in\Omega} |\mathcal{G}_1(S,t)|$, *and*

$$\mathbb{A} \;=\; \begin{cases} \mathbb{A}^*, & U = 0, \\ min\left\{\mathbb{A}^*, \left(\dfrac{L\Gamma(\tau+1)\xi^{\tau}}{U}\right)^{\frac{1}{\tau}}\right\}, & else. \end{cases} \tag{5.3}$$

Then, there exists a function $S \in C[0,\mathbb{A}]$ *that solves the IVP (5.1). Here,* $C[0,\mathbb{A}]$ *is the set of all continuous functions within the closed interval* $[0,\mathbb{A}]$.

Lemma 3. *[14] Let us consider that the hypotheses of Theorem 3 is true. The function* $S \in C[0,\mathbb{A}]$ *is a solution of the IVP (5.1) iff, it is a solution of the non-linear Volterra integral Eq (5.2).*

Proof of Theorem 3. If $U = 0$, then $\mathcal{G}_1(S,t) = 0\ \forall\ (t,S) \in \Omega$. Here, it is obvious by the method of direct substitution that the solution of the IVP (5.1) is the function $S : [0,\mathbb{A}] \to \mathbb{R}$. Therefore, in this case, the solution exists.

For $U \neq 0$, Lemma 3 is applied now to prove that IVP (5.1) is equivalent to the Volterra integral Eq (5.2). Define the set $\mathcal{M} = \{S \in C[0,\mathbb{A}] :\| S - S_0 \|_{\infty} \leq L\}$. It is obvious that $\mathcal{M}$ is a convex subset of the Banach space of all continuous functions on $[0,\mathbb{A}]$ and closed, equipped with the Chebyshev norm. This gives the idea that the set $\mathcal{M}$ is a non-void Banach space, since $S_0 \in \mathcal{M}$. An operator $\mathcal{E}$ is now defined on the set $\mathcal{M}$ by

$$(\mathcal{E}S)(t) \;=\; S_0 + \frac{\xi^{1-\tau}}{\Gamma(\tau)} \int_0^t z^{\xi-1} \left(t^{\xi} - z^{\xi}\right)^{\tau-1} \mathcal{G}_1(S,z)\, dz. \tag{5.4}$$

Afterwards, Eq (5.2) can be written as $S = \mathcal{E}S$, and thus it needs to be shown that $\mathcal{E}$ has a fixed point. This is done by Schauder's Second Fixed Point Theorem. At first, it will be shown that $\mathcal{M}$ is closed, that is, $\mathcal{E}S \in \mathcal{M}$ for all $S \in \mathcal{M}$. For $0 \leq t_1 \leq t_2 \leq \mathbb{A}$,

$$\begin{aligned} &|(\mathcal{E}S)(t_1) - (\mathcal{E}S)(t_2)| \\ &= \frac{\xi^{1-\tau}}{\Gamma(\tau)} \Big| \int_0^{t_1} z^{\xi-1} \left(t_1^{\xi} - z^{\xi}\right)^{\tau-1} \mathcal{G}_1(S,z)\, dz - \int_0^{t_2} z^{\xi-1} \left(t_2^{\xi} - z^{\xi}\right)^{\tau-1} \mathcal{G}_1(S,z)\, dz \Big| \end{aligned}$$

$$= \frac{\xi^{1-\tau}}{\Gamma(\tau)} \left| \int_0^{t_1} \left[\left(t_1^\xi - z^\xi\right)^{\tau-1} - \left(t_2^\xi - z^\xi\right)^{\tau-1} \right] z^{\xi-1} \mathcal{G}_1(S,z)\, dz + \int_{t_1}^{t_2} z^{\xi-1} \left(t_2^\xi - z^\xi\right)^{\tau-1} \mathcal{G}_1(S,z)\, dz \right|.$$

Therefore, we now have

$$|(\mathcal{E}S)(t_1) - (\mathcal{E}S)(t_2)| \leq \frac{U\xi^{\tau-1}}{\Gamma(\tau)} \left(\int_0^{t_1} |\left(t_1^\xi - z^\xi\right)^{\tau-1} - \left(t_2^\xi - z^\xi\right)^{\tau-1} | z^{\xi-1} dz + \int_{t_1}^{t_2} z^{\xi-1} \left(t_2^\xi - z^\xi\right)^{\tau-1} dz \right). \quad (5.5)$$

In Inequality (5.5), the second integral in the R.H.S. has the value $\frac{1}{\xi\tau}\left(t_2^\xi - z^\xi\right)^\tau$. We consider two cases, viz. $\tau < 1$ and $\tau = 1$, for the first integral in Inequality (5.5). For $\tau = 1$, zero is the value of said integral, and we have $\left(t_1^\xi - z^\xi\right)^{\tau-1} \geq \left(t_2^\xi - z^\xi\right)^{\tau-1}$ for the case $\tau < 1$. Thus,

$$\begin{aligned} \int_0^{t_1} |\left(t_1^\xi - z^\xi\right)^{\tau-1} - \left(t_2^\xi - z^\xi\right)^{\tau-1} | z^{\xi-1} dz &= \int_0^{t_1} \left[\left(t_1^\xi - z^\xi\right)^{\tau-1} - \left(t_2^\xi - z^\xi\right)^{\tau-1} \right] z^{\xi-1} dz \\ &= \frac{1}{\xi\tau}\left(t_1^\xi \tau - t_2^\xi \tau\right) + \frac{1}{\xi\tau}\left(t_2^\xi - t_1^\xi\right)^\tau \\ &\leq \frac{1}{\xi\tau}\left(t_2^\xi - t_1^\xi\right)^\tau. \end{aligned}$$

Using the above results, if $\tau \leq 1$, we can have

$$|(\mathcal{E}S)(t_1) - (\mathcal{E}S)(t_2)| \leq \frac{2U}{\xi^\tau \Gamma(\tau+1)} \left(t_2^\xi - t_1^\xi\right)^\tau. \quad (5.6)$$

In either case, the R.H.S. expression of Inequality (5.6) converges to zero as t_2 tends to t_1, and this suffices the proof that $\mathcal{E}S$ is a continuous function, since S_0 from Eq (5.1) is itself continuous. It is also a fact that for $S \in \mathcal{M}$ and $t \in [0, A]$,

$$\begin{aligned} |(\mathcal{E}S)(t) - S_0| &= \frac{\xi^{\tau-1}}{\Gamma(\tau)} \left| \int_0^t z^{\xi-1} \left(t^\xi - z^\xi\right)^{\tau-1} \mathcal{G}_1(S,z)\, dz \right| \\ &\leq \frac{U}{\xi^\tau \Gamma(\tau+1)} t^{\xi\tau} \leq \frac{U}{\xi^\tau \Gamma(\tau+1)} A^{\xi\tau} \leq \frac{U}{\xi^\tau \Gamma(\tau+1)} . \frac{\xi^\tau L \Gamma(\tau+1)}{U}, \end{aligned}$$

by the definition of $\mathbb{A}$ from Eq (5.3). Thus, we have $|(\mathcal{E}S)(t) - S_0| \leq L$. Therefore, it can be said that $\mathcal{E}S \in \mathcal{M}$ if $S \in \mathcal{M}$, i.e., S is an into mapping from the set $\mathcal{M}$ to S.

Now, we will show that the set $\mathcal{E}(\mathcal{M}) := \{\mathcal{E}\bar{m} : \bar{m} \in \mathcal{M}\}$ is relatively compact by the Arzelá-Ascoli Theorem. We first prove that the set $\mathcal{E}(\mathcal{M})$ is bounded uniformly by letting $\alpha \in \mathcal{E}(\mathcal{M})$. For all $t \in [0, \mathbb{A}]$, we see that

$$\begin{aligned} |\alpha(t)| &= |(\mathcal{E}\mathcal{M})(t)| \\ &\leq \|S_0\|_\infty + \frac{\xi^{1-\tau}}{\Gamma(\tau)} \int_0^t z^{\xi-1} \left(t^\xi - z^\xi\right)^{\tau-1} |\mathcal{G}_1(S,z)| dz \\ &\leq \|S_0\|_\infty + \frac{1}{\xi^\tau \Gamma(\tau+1)} U A^\tau \leq \|S_0\|_\infty + L, \end{aligned}$$

and this is the property of boundedness that we have wanted. The property of equicontinuity can be evaluated from Inequality (5.6). For $t_1, t_2 \in [0, \mathbb{A}]$ and $\tau \leq 1$, we get

$$|(\mathcal{E}S)(t_1 - t_2)| \leq \frac{2U}{\xi^\tau \Gamma(\tau+1)} \left(t_2^\xi - t_1^\xi\right)^\tau = \frac{2U}{\Gamma(\tau+1)} (t_2 - t_1)^\tau \theta^{\tau(\xi-1)},$$

for some $\theta \in [t_1, t_2] \subset [0, \mathbb{A}]$. So, we have

$$|(\mathcal{E}S)(t_1) - (\mathcal{E}S)(t_2)| \leq U'\rho + \frac{2U}{\Gamma(\tau+1)} \rho^\tau A^{\tau(\xi-1)}, \tag{5.7}$$

if $|t_1 - t_2| < \rho$, for some $U' > 0$, since in the interval $[0, \mathbb{A}]$, S_0 is uniformly continuous. The set $\mathcal{E}(\mathcal{M})$ is equicontinuous as, we note that the expression in the R.H.S. of (5.7) is not dependent on S, t_1 and t_2. The Arzelá-Ascoli Theorem gives that the set $\mathcal{E}(\mathcal{M})$ is relatively compact in either case, and therefore, by Schauder's Second Fixed Point Theorem, we can say that $\mathcal{E}$ possesses a fixed point. This fixed point is the required positive solution of the IVP (5.1).

Similarly, we can show that for other state variables the solution exists. □

5.2. Boundedness of solution

We seek the help of Eq (5.4), where the property of operator $\mathcal{E}$ is defined. Let $S_1, S_2 \in C[0, \mathbb{A}] \subset [0, t]$ and assume that there exists a constant $\mathcal{L} > 0$, which is not dependent on S_1, S_2 and t, such that $|\mathcal{G}_1(S_1, t) - \mathcal{G}_2(S_2, t)| \leq \mathcal{L}|S_1 - S_2|$ for all $t \in [0, \mathbb{A}]$. Doing so, we can have

$$\begin{aligned}
\|\mathcal{E}S_1 - \mathcal{E}S_2\|_{\mathcal{L}_\infty[0,\mathbb{A}]} &= \frac{\xi^{1-\tau}}{\Gamma(\tau)} \sup_{0\leq w\leq t} \left| \int_0^w \left(w^\xi - z^\xi\right)^{\tau-1} z^{\xi-1} \left[\mathcal{G}_1\left(S_1(z), z\right) - \mathcal{G}_1\left(S_2(z), z\right)\right] dz \right| \\
&\leq \frac{\mathcal{L}\xi^{1-\tau}}{\Gamma(\tau)} \sup_{0\leq w\leq t} \left| \int_0^w \left(w^\xi - z^\xi\right)^{\tau-1} z^{\xi-1} |S_1(z) - S_2(z)| dz \right| \\
&\leq \frac{\mathcal{L}\xi^{1-\tau}}{\Gamma(\tau)} \|S_1 - S_2\|_{\mathcal{L}_\infty[0,\mathbb{A}]} \sup_{0\leq w\leq t} \left| \int_0^w \left(w^\xi - z^\xi\right)^{\tau-1} z^{\xi-1} dz \right| \\
&\leq \frac{\mathcal{L}\xi^{1-\tau}}{\Gamma(\tau)} \|S_1 - S_2\|_{\mathcal{L}_\infty[0,\mathbb{A}]} \sup_{0\leq w\leq t} \left| \frac{1}{\xi\tau} \left[\left(w^\xi - z^\xi\right)^\tau\right]_0^w \right|.
\end{aligned}$$

Therefore, we have $\|\mathcal{E}S_1 - \mathcal{E}S_2\|_{\mathcal{L}_\infty[0,\mathbb{A}]} = \dfrac{\mathcal{L}\left(\frac{t^\xi}{\xi}\right)^\tau}{\Gamma(\tau+1)} \|S_1 - S_2\|_{\mathcal{L}_\infty[0,t]}$, and following which we have the next theorem.

Theorem 4. *[14] Let $\mathcal{E}$ and $\mathcal{M}$ be defined as in the proof of Theorem 3. Suppose $\vartheta \in \mathbb{N}_0$, $t \in [0, \mathbb{A}]$, with $S, \bar{S} \in \mathcal{M}$. Let $\mathcal{G}_1$ suffices the Lipschitz condition with the Lipschitz constant $\mathcal{L}$. Then,*

$$\|\mathcal{E}^\vartheta S - \mathcal{E}^\vartheta \bar{S}\|_{\mathcal{L}_\infty[0,t]} \leq \frac{\mathcal{L}^\vartheta \left(\frac{t^\xi}{\xi}\right)^{\tau\vartheta}}{\Gamma(\tau\vartheta+1)} \|S - \bar{S}\|_{\mathcal{L}_\infty[0,t]}. \tag{5.8}$$

Theorem 5. *Let $S_0 \in \mathbb{R}$, $L > 0$ and $\mathbb{A}^* > 0$. Also, suppose $0 < \tau \leq 1$, and $k = \lceil \tau \rceil$. Define the set $\mathcal{G}_1$ as in Theorem 3 and say the continuous function $\mathcal{G}_1 : \mathcal{G} \to \mathbb{R}$ satisfies a Lipschitz condition with respect to the second variable, i.e., $|\mathcal{G}_1(S_1, t) - \mathcal{G}_1(S_2, t)| \leq L|S_1 - S_2|$ for some positive constant L not dependent on S_1, S_2 and t. Then, there exists a unique solution $S \in C[0, \mathbb{A}]$ for the IVP (5.1).*

Proof. As per Theorem 3, the IVP (5.1) has a positive solution. We seek the help of Theorem 4 in order to prove the uniqueness criteria. In particular, we utilize the operator $\mathcal{E}$ as stated in Eq (5.4), and it maps the non-void, convex and closed set $\mathcal{M} = \{S \in C[0, \mathbb{A}] : \|S - S_0\|_\infty \leq L\}$ to itself. In order to show that $\mathcal{E}$ has a unique fixed point, we now use Weissinger's Fixed Point Theorem. Let $\vartheta \in \mathbb{N}_0$, $t \in [0, \mathbb{A}]$ and $S_1, S_2 \in \mathcal{M}$. Afterwards, using relation (5.8) and taking the help of the Chebyshev norms on the interval $[0, \mathbb{A}]$, we now have

$$\|\mathcal{E}^\vartheta S - \mathcal{E}^\vartheta \bar{S}\|_\infty \leq \frac{L^\vartheta \left(\frac{t^\xi}{\xi}\right)^{\tau\vartheta}}{\Gamma(\tau\vartheta + 1)} \|S - \bar{S}\|_\infty.$$

Let $w_\vartheta = \dfrac{L^\vartheta \left(\frac{\mathbb{A}^\xi}{\xi}\right)^{\tau\vartheta}}{\Gamma(\tau\vartheta + 1)}$. We have to prove that the series $\displaystyle\sum_{\vartheta=0}^{\infty} w_\vartheta$ is convergent, in order to apply the theorem. It is obvious from noticing that w_ϑ is simply the power series representation of the Mittag-Leffler function $\mathcal{E}^*_\tau\left(L\left(\frac{T^\xi}{\xi}\right)^\tau\right)$; hence, the series is convergent.

Similarly, we can use same argument to show uniqueness for other state variables. □

By the theorems depicted in Section 5, it can be easily understood that the solutions of the state variables involved in the system are bounded.

6. The basic reproduction number, $\mathcal{R}_0$

For real life problems and by dint of biological restrictions, only admissible solutions of any IVP (here, the systems (3.1) and (3.2) with the initial conditions) ought to be non-negative. This has been put clearly in Sections 4 and 5. The analysis of the basic reproduction number of a system of fractional order differential equations and that of a system of ordinary differential equations are the same [12].

The Basic Reproduction Number is an important number which determines the mean of secondary infections that happens during introduction of an infected being into a herd of susceptible populace. The detailed calculations for finding it by the next generation matrix method, see [9, 27]. Generally, this number can explain pandemiologically broadly into two ways. If the number is less than unity, then infection will tend to reduce in time because the CoVID-19 virus will become inactive. On the other hand, if it is greater than unity, then infection will spread and therefore the infection will spread rapidly. For the system (3.1), the basic reproduction number is denoted and given as

$$\mathcal{R}_0 = \frac{\beta\lambda\sqrt{\mu + d} + \sqrt{\beta\lambda\{4\eta d(\eta + d) + \beta\lambda(\mu + d)\}}}{2d(\eta + d)\sqrt{\mu + d}},$$

which is clearly a differential function as long as the denominator is not zero.

As per our assumption, an asymptomatic individual reflects symptoms of CoVID-19 disease with rate η. The direction of spread is given by the term η in $\mathcal{R}_0$. Also, β is the rate at which the infection is spreading from the susceptible to the asymptomatic populace, and the natural human natality rate is λ. It can be stated that the term $\beta\lambda$ represents secondary infections that are seen in susceptible individuals. Therefore, $\mathcal{R}_0$ is biologically meaningful. We have focused on λ, η and β as we are keenly interested in the spread direction. The remaining parameters, involved in this basic reproduction number, are dealt with the absolute values.

7. Sensitivity analysis of $\mathcal{R}_0$

With respect to spread of infection, sensitivity analysis provides ideas about how every parameter involved in the mathematical model of that disease dynamics is vital. Information of such kinds is not only important for designing experiments, but also to collect data and relaxation in modeling the complicated non-linear disease models. As the collections of data are concerned, errors in assumed values of parameters cannot be denied. Thus, sensitivity analysis is usually emphasized in determining accuracies of the presumptions of values of parameters. Sensitivity analysis of the basic reproduction number is used to identify parameters that may or can have great impact on it and therefore must be targeted by strategic interventions. A parameter having high sensitivity should be carefully handled, as an infinitesimal change in it may cause a huge quantitative change in $\mathcal{R}_0$.

The sensitivity indices measure the changes that are relative to the parameters. We seek the help of the normalized forward sensitivity index [26, 29] of $\mathcal{R}_0$. For the differentiable function $\mathcal{R}_0 \equiv \mathcal{R}_0(u)$, it is denoted and defined as $\gamma_u^{\mathcal{R}_0} = \dfrac{\partial \mathcal{R}_0}{\partial u} \times \dfrac{u}{\mathcal{R}_0}$. Here, u is an abstract form of any variable present in the expression of $\mathcal{R}_0$. The sensitive indices of $\mathcal{R}_0$ with respect to the parameters λ, β and η are given in Table 2.

Table 2. Sensitivity of $\mathcal{R}_0$ calculated for the parameter's values presented in Table 1, as per the expression of $\mathcal{R}_0$.

$Parameters(u) \rightarrow$	λ	η	β
$\gamma_u^{\mathcal{R}_0} \rightarrow$	$0.504408 \approx 0.5$	$0.0300107 \approx 0.03$	$0.504408 \approx 0.5$

If there is a 1% increment in λ, then $\mathcal{R}_0$ increases by 0.5%. Next, if η increases or decreases by 1%, then there will be a corresponding change in $\mathcal{R}_0$ of 0.03%. Following the same argument, an increment or decrement of 1% in β will result in a corresponding change in $\mathcal{R}_0$ of 0.5%. Controlling λ and β depend upon the seriousness of precautionary measures that are defined as per the government guidelines. This implies that amongst the three parameters, the most sensitive parameter is η, as symptoms in an asymptomatic are not visible until they show some symptoms of the infection.

8. Numerical schemes, simulations and results

In this section, we provide the numerical schemes in brief by which the integer order model (3.1) and the fractional order model (3.2) are solved. The section also has descriptive results obtained by solving the aforementioned models.

8.1. Ms-DTM scheme

The operation table of differential transformations of some standard functions can be found in Odibat *et al*. [22]. To recapitulate, the non-linear initial problem

$$\mathcal{J}(t, x, x', \cdots x^{(r)}) \quad = \quad 0$$

is considered with some constraints $x^{(q)}(0) = b_q$, for $q = 0, 1, \cdots, (r-1)$.

Let $[0, B]$ be the interval in which the intention is to find the solution of the IVP $\mathcal{J} = 0$. The nearby solutions of this IVP, by the DTM, can be simplified by the series

$$x(t) = \sum_{n=0}^{N} u_n t^n \qquad t \in [0, B].$$

The interval $[0, B]$ is now divided into $\mathbb{M}$ subintervals $[t_{m-1}, t_m]$, where $m = 1, 2, \cdots, \mathbb{M}$ of same length $h = \frac{B}{\mathbb{M}}$ by using the relations $t_m = hm$. The DTM is now induced to the IVP $\mathcal{J} = 0$ over the interval $[0, t_1]$, and thus we obtain the approximate solution

$$x_1(t) = \sum_{n=0}^{\mathcal{K}} u_{1n} t^n, \qquad t \in [0, t_1],$$

with the boundary conditions as $x_1^{(q)}(0) = b_q$. The boundary conditions $x_m^{(q)}(t_{m-1}) = x_{m-1}^{(q)}(t_{m-1})$ at each sub-interval $[t_{m-1}, t_m]$ for $m \geq 2$ are used, and the DTM is applied to the IVP $\mathcal{J} = 0$ over the interval $[t_{m-1}, t_m]$. The process is iterated so that a sequence of approxximated solutions $x_m(t)$, $m = 1, 2, \cdots, \mathbb{M}$ is generated for the solutions $x(t)$,

$$x_m(t) = \sum_{n=0}^{\mathcal{K}} u_{mn} (t - t_{m-1})^n, \qquad t \in [t_m, t_{m+1}],$$

where $\mathcal{K}.\mathbb{M} = N$. Therefore, the Ms-DTM takes the following solution:

$$x(t) = \begin{cases} x_1(t), & t \in [0, t_1], \\ x_2(t), & t \in [t_1, t_2], \\ \ldots & \\ x_{\mathbb{M}}(t), & t \in [t_{\mathbb{M}-1}, t_{\mathbb{M}}]. \end{cases} \tag{8.1}$$

Applying the DTM to the system (3.1), we get the following set of equations:

$$\begin{aligned} (\mathcal{K}+1)S(\mathcal{K}+1) &= \lambda\delta(\mathcal{K}) - \beta \sum_{n=0}^{\mathcal{K}} S(n)\{A(\mathcal{K}-n) + I(\mathcal{K}-n)\} - dS(\mathcal{K}), \\ (\mathcal{K}+1)A(\mathcal{K}+1) &= \beta \sum_{n=0}^{\mathcal{K}} S(n)\{A(\mathcal{K}-n) + I(\mathcal{K}-n)\} - (\eta + d)A(\mathcal{K}), \\ (\mathcal{K}+1)I(\mathcal{K}+1) &= \eta A(\mathcal{K}) - (\mu + d)I(\mathcal{K}), \end{aligned} \tag{8.2}$$

where $S(\mathcal{K})$, $A(\mathcal{K})$ and $I(\mathcal{K})$ are the differential transformation of $S(t)$, $A(t)$ and $I(t)$, respectively. The initial condition of the system (8.2) is the same as that of the IVP (3.1). Now, we apply the Ms-DTM as per the approach such that $S(t)$, $A(t)$ and $I(t)$ satisfy the relation (8.1). Therefore, $S_m(l)$, $A_s(l)$ and $I_s(l)$ satisfy the following recursive relations:

$$\begin{aligned} (\mathcal{K}+1)S_m(\mathcal{K}+1) &= \lambda\delta(\mathcal{K}) - \beta \sum_{n=0}^{\mathcal{K}} S_m(n)\{A_m(\mathcal{K}-n) + I_m(\mathcal{K}-n)\} - dS_m(\mathcal{K}), \\ (\mathcal{K}+1)A_m(\mathcal{K}+1) &= \beta \sum_{n=0}^{\mathcal{K}} S_m(n)\{A_m(\mathcal{K}-n) + I_m(\mathcal{K}-n)\} - (\eta + d)A_m(\mathcal{K}), \\ (\mathcal{K}+1)I_m(\mathcal{K}+1) &= \eta A_m(\mathcal{K}) - (\mu + d)I_m(\mathcal{K}), \end{aligned} \tag{8.3}$$

subject to the mentioned conditions, which are:

i) $S_0(0) = S_0, A_0(0) = A_0, I_0(0) = I_0$;
ii) $S_m(0) = S_{m-1}(0), A_m(0) = A_{m-1}(0), I_m(0) = I_{m-1}(0)$.

8.2. Predictor-corrector scheme and its stability

To develop the PC method for the IVP (5.1), we will follow the procedure cited in Odibat *et al*. [22] with some little alterations, and afterwards a study of the stability of the PC method will be done. For doing so, we initiate from the equivalent Volterra integral Eq (5.2), which is

$$S(t) = S_0 + \frac{\xi^{1-\tau}}{\Gamma(\tau)} \int_0^t z^{\xi-1} \left(t^\xi - z^\xi\right)^{\tau-1} \mathcal{G}_1(S, z)\, dz. \tag{8.4}$$

We assume that $\mathcal{G}_1$ is a function such that on some arbitrary interval $[0, \mathbb{A}]$ its unique solution exists. So, the 4-step PC algorithm is as follows.

Step I. Divide the interval $[0, \mathbb{A}]$ into $\mathcal{N}$ sub-intervals $\left\{\left[t_j, t_{j+1}\right], j = 0, 1, 2, \cdots, \mathcal{N}-1\right\}$ by taking the help of mesh points

$$\begin{cases} t_0 = 0, \\ t_{j+1} = \left(t_j^\xi + c\right)^{\frac{1}{\xi}}; j = 0, 1, 2, \cdots, \mathcal{N}-1, \end{cases} \tag{8.5}$$

where $c = \frac{\mathbb{A}^\xi}{\mathcal{N}}$.

Step II. Generate the approximations S_{j+1} $(j = 0, 1, 2, \cdots, \mathcal{N}-1)$, to evaluate the IVP (5.1) numerically. The introductory step, supposing that the approximations $S_\vartheta \approx S(t_\vartheta)$ $(\vartheta = 1, 2, 3, \cdots, j)$ have been solved, is that we need to achieve the approximation $S_{j+1} \approx S(t_{j+1})$ by means of the integral equation

$$S(t_{j+1}) = S_0 + \frac{\xi^{1-\tau}}{\Gamma(\tau)} \int_0^{t_{j+1}} z^{\xi-1} \left(t_{j+1}^\xi - z^\xi\right)^{\tau-1} \mathcal{G}_1(S, z)\, dz. \tag{8.6}$$

We let $\alpha = z^\xi$, and we get

$$S(t_{j+1}) = S_0 + \frac{\xi^{-\tau}}{\Gamma(\tau)} \int_0^{t_{j+1}^\xi} \left(t_{j+1}^\xi - \alpha\right)^{\tau-1} \mathcal{G}_1\left(\alpha^{\frac{1}{\xi}}, S(\alpha^{\frac{1}{\xi}})\right) d\alpha, \tag{8.7}$$

that is,

$$S(t_{j+1}) = S_0 + \frac{\xi^{-\tau}}{\Gamma(\tau)} \sum_{\vartheta=0}^{j} \int_{t_\vartheta^\xi}^{t_{j+1}^\xi} \left(t_{j+1}^\xi - \alpha\right)^{\tau-1} \mathcal{G}_1\left(\alpha^{\frac{1}{\xi}}, S(\alpha^{\frac{1}{\xi}})\right) d\alpha. \tag{8.8}$$

Step III. With regard to the weight function $\left(t_{j+1}^\xi - \alpha\right)^{\tau-1}$, we use the trapezoidal quadrature rule to approximate the integrals that emerge in the R.H.S. of Eq (8.8), replacing the map $\mathcal{G}_1\left(\alpha^{\frac{1}{\xi}}, S(\alpha^{\frac{1}{\xi}})\right)$ by its piecewise linear interpolant with nodes selected at t_ϑ^ξ $(\vartheta = 0, 1, 2, \cdots, j+1)$. Then, we get

$$\int_{t_\vartheta^\xi}^{t_{j+1}^\xi} \left(t_{j+1}^\xi - \alpha\right)^{\tau-1} \mathcal{G}_1\left(\alpha^{\frac{1}{\xi}}, S(\alpha^{\frac{1}{\xi}})\right) d\alpha \approx \frac{c^\tau}{\tau(\tau+1)} \left(\Im_1 + \Im_2\right), \tag{8.9}$$

where

$$\begin{aligned}\Im_1 &= \left((j-\vartheta)^{\tau+1}-(j-\vartheta-\tau)(j-\vartheta+1)^{\tau}\right)\mathcal{G}_1\left(S(t_\vartheta),t_\vartheta\right),\\ \Im_2 &= \left((j-\vartheta+1)^{\tau+1}-(j-\vartheta+\tau+1)(j-\vartheta)^{\tau}\right)\mathcal{G}_1\left(S(t_{\vartheta+1}),t_{\vartheta+1}\right).\end{aligned}$$

Therefore, using the aforementioned approximations to Eq (8.8), we get the corrector formula for $S(t_{j+1})$, $j=0,1,2,\cdots,\mathcal{N}-1$,

$$S(t_{j+1}) \approx S_0+\frac{\xi^{-\tau}c^{\tau}}{\Gamma(\tau+2)}\left[\sum_{\vartheta=0}^{j}\Delta_{\vartheta,j+1}\mathcal{G}_1\left(t_\vartheta,S(t_\vartheta)\right)+\mathcal{G}_1\left(t_{j+1},S(t_{j+1})\right)\right], \tag{8.10}$$

where

$$\Delta_{\vartheta,j+1} = \begin{cases} j^{\tau+1}-(j-\tau)(j+1)^{\tau}, & \vartheta=0,\\ (j-\vartheta+2)^{\tau+1}+(j-\vartheta)^{\tau+1}-2(j-\vartheta+1)^{\tau+1}, & \vartheta\in[1,j].\end{cases} \tag{8.11}$$

Step IV. Substitute $S(t_{j+1})$ of the R.H.S. of the relation (8.10) by the predictor term $S^{\mathcal{P}}(t_{j+1})$ that can be achieved by applying the one-step Adams-Bashforth method to the integral, Eq (8.4). In this scenario, by substituting the function $\mathcal{G}_1\left(\alpha^{\frac{1}{\xi}},S(\alpha^{\frac{1}{\xi}})\right)$ by $\mathcal{G}_1\left(t_\vartheta,S(t_\vartheta)\right)$ at every integral in Eq (8.8), we obtain

$$\begin{aligned}S^{\mathcal{P}}(t_{j+1}) &\approx S_0+\frac{\xi^{-\tau}}{\Gamma(\tau)}\sum_{\vartheta=0}^{j}\int_{t_\vartheta^{\xi}}^{t_{j+1}^{\xi}}\left(t_{j+1}^{\xi}-\alpha\right)^{\tau-1}\mathcal{G}_1\left(t_\vartheta,S(t_\vartheta)\right)d\alpha\\ &= S_0+\frac{\xi^{-\tau}c^{\tau}}{\Gamma(\tau+1)}\sum_{\vartheta=0}^{j}\left[(j+1-\vartheta)^{\tau}-(j-\vartheta)^{\tau}\right]\mathcal{G}_1\left(t_\vartheta,S(t_\vartheta)\right).\end{aligned} \tag{8.12}$$

Thus, an adaptive PC algorithm, for calculating the approximation $S_{j+1}\approx S(t_{j+1})$, is wholly depicted by the formula

$$S_{j+1} \approx S_0+\frac{\xi^{-\tau}c^{\tau}}{\Gamma(\tau+2)}\left[\sum_{\vartheta=0}^{j}\Delta_{\vartheta,j+1}\mathcal{G}_1\left(t_\vartheta,S_\vartheta\right)+\mathcal{G}_1\left(t_{j+1},S_{j+1}^{\mathcal{P}}\right)\right], \tag{8.13}$$

where $S_\vartheta\approx S(t_\vartheta)$, $\vartheta=0,1,2,\cdots,j$, and $S_{j+1}^{\mathcal{P}}\approx S^{\mathcal{P}}(t_{j+1})$ can be calculated as depicted in Eq (8.12) with the weights $\Delta_{\vartheta,j+1}$ being defined as per (8.13).

In the same manner, the solution of the other equations of IVP (5.1) may be written as follows:

$$\begin{aligned}A_{j+1} &\approx A_0+\frac{\xi^{-\tau}c^{\tau}}{\Gamma(\tau+2)}\left[\sum_{\vartheta=0}^{j}\Delta_{\vartheta,j+1}\mathcal{G}_2\left(t_\vartheta,A_\vartheta\right)+\mathcal{G}_2\left(t_{j+1},A_{j+1}^{\mathcal{P}}\right)\right],\\ I_{j+1} &\approx I_0+\frac{\xi^{-\tau}c^{\tau}}{\Gamma(\tau+2)}\left[\sum_{\vartheta=0}^{j}\Delta_{\vartheta,j+1}\mathcal{G}_3\left(t_\vartheta,I_\vartheta\right)+\mathcal{G}_3\left(t_{j+1},I_{j+1}^{\mathcal{P}}\right)\right],\end{aligned} \tag{8.14}$$

where

$$\begin{aligned}A_{t_{j+1}}^{\mathcal{P}} &\approx A_0+\frac{\xi^{-\tau}c^{\tau}}{\Gamma(\tau+1)}\sum_{\vartheta=0}^{j}\left[(j+1-\vartheta)^{\tau}-(j-\vartheta)^{\tau}\right]\mathcal{G}_2\left(t_\vartheta,A(t_\vartheta)\right),\\ I_{t_{j+1}}^{\mathcal{P}} &\approx I_0+\frac{\xi^{-\tau}c^{\tau}}{\Gamma(\tau+1)}\sum_{\vartheta=0}^{j}\left[(j+1-\vartheta)^{\tau}-(j-\vartheta)^{\tau}\right]\mathcal{G}_3\left(t_\vartheta,I(t_\vartheta)\right).\end{aligned} \tag{8.15}$$

Theorem 6 (Stability theorem)**.** *The numerical method of (8.12) and (8.13) is conditionally stable under the assumption if $\mathcal{G}_1(S,t)$ in IVP (5.1) satisfies the Lipschitz condition, and S_ϑ ($\vartheta = 1,2,3,\cdots,j+1$) are the solutions of the first approximations of the PC methodology (8.12) and (8.13).*

Proof. Let $\bar{S}_0$, $\bar{S}_\vartheta$ ($\vartheta = 0,1,2,\cdots,j+1$) and $\bar{S}^{\mathcal{P}}_{j+1}$ be perturbations of S_0, S_ϑ and $S^{\mathcal{P}}_{j+1}$, respectively. Then, we get the following perturbation equations with the help of Eqs (8.10) and (8.12):

$$\bar{S}^{\mathcal{P}}_{j+1} = \bar{S}_0 + \frac{\xi^{-\tau}c^\tau}{\Gamma(\tau+1)}\sum_{\vartheta=0}^{j}\mu_{\vartheta,j+1}\Big(\mathcal{G}_1(t_\vartheta, S_\vartheta+\bar{S}_\vartheta) - \mathcal{G}_1(t_\vartheta, S_\vartheta)\Big),$$

where $\mu_{\vartheta,j+1} = [(j+1-\vartheta)^\tau - (j-\vartheta)^\tau]$, and

$$\begin{aligned}\bar{S}_{j+1} &= S_0 + \frac{\xi^{-\tau}c^\tau}{\Gamma(\tau+2)}\Big(\mathcal{G}_1(t_{j+1}, S^{\mathcal{P}}_{j+1}+\bar{S}^{\mathcal{P}}_{j+1}) - \mathcal{G}_1(t_{j+1}, S^{\mathcal{P}}_{j+1})\Big)\\ &\quad + \frac{\xi^{-\tau}c^\tau}{\Gamma(\tau+2)}\sum_{\vartheta=0}^{j}\Delta_{\vartheta,j+1}\Big(\mathcal{G}_1(t_\vartheta, S_\vartheta+\bar{S}_\vartheta) - \mathcal{G}_1(t_\vartheta, S_\vartheta)\Big).\end{aligned}$$

We now use the Lipschitz condition, and thus obtain

$$|\bar{S}_{j+1}| \leq \pi_0 + \frac{\xi^{-\tau}c^\tau}{\Gamma(\tau+2)}\left(|\bar{S}^{\mathcal{P}}_{j+1}| + \sum_{\vartheta=0}^{j}\Delta_{\vartheta,j+1}|\bar{S}_\vartheta|\right),$$

where $\pi_0 = \max\limits_{0\leq j\leq \mathcal{N}}\left\{|\bar{S}_0| + \frac{\xi^{-\tau}c^\tau\Delta_{j,0}}{\Gamma(\tau+2)}|\bar{S}_0|\right\}$. Also, from Eq (3.18) in Li [18], we get

$$|\bar{S}^{\mathcal{P}}_{j+1}| \leq \nu_0 + \frac{\xi^{-\tau}c^\tau}{\Gamma(\tau+1)}\sum_{\vartheta=1}^{j}\mu_{\vartheta,j+1}|\bar{S}_\vartheta|,$$

where $\nu_0 = \max\limits_{0\leq j\leq \mathcal{N}}\left\{|\bar{S}_0| + \frac{\xi^{-\tau}c^\tau\mu_{j,0}}{\Gamma(\tau+1)}|\bar{S}_0|\right\}$. Eventually, we get

$$\begin{aligned}|\bar{S}_{j+1}| &\leq \iota_0 + \frac{\xi^{-\tau}c^\tau}{\Gamma(\tau+2)}\left(\frac{\xi^{-\tau}c^\tau}{\Gamma(\tau+1)}\sum_{\vartheta=1}^{j}\mu_{\vartheta,j+1}|\bar{S}_\vartheta| + \sum_{\vartheta=1}^{j}\Delta_{\vartheta,j+1}|\bar{S}_\vartheta|\right)\\ &\leq \iota_0 + \frac{\xi^{-\tau}c^\tau}{\Gamma(\tau+2)}\sum_{\vartheta=1}^{j}\left(\frac{\xi^{-\tau}c^\tau}{\Gamma(\tau+1)}\mu_{\vartheta,j+1} + \Delta_{\vartheta,j+1}\right)|\bar{S}_\vartheta|\\ &\leq \iota_0 + \frac{\xi^{-\tau}c^\tau\mathfrak{C}_{\tau,2}}{\Gamma(\tau+2)}\sum_{\vartheta=1}^{j}(j+1-\vartheta)^{\tau-1}|\bar{S}_\vartheta|,\end{aligned}$$

where $\iota_0 = \max\left\{\pi_0 + \frac{\xi^{-\tau}c^\tau\Delta_{j+1,j+1}}{\Gamma(\tau+2)}\nu_0\right\}$. $\mathfrak{C}_{\tau,2}$ is a positive constant which completely depends on τ, by Lemma 1, and c is assumed to be infinitesimally small. Using Lemma 2, we conclude that $|\bar{S}_{j+1}| \leq \mathfrak{C}\times\iota_0$.

Similarly, it can also be shown for the other state variables. □

8.3. Results obtained from simulation

We have taken the CoVID-19 pandemic model from Zamir *et al*. [29]. To do the numerical simulations, we have used the parameter values, given in Table 1. The initial conditions of the populations are estimated from Erturk *et al*. [10], and are as follows: $S_0 = 11 \times 10^6$, $A_0 = 3$, and $I_0 = 4$. Figure 2 provides the behavioural presentation of results that are achieved by the projected solution process for the state variables at various values of $\tau = 1, 0.98, 0.95, 0.92$ and at a constant value of $\xi = 1.25$. We see that for the susceptible and asymptomatic populaces, the fractional order model has almost same nature from $\tau \in [0.98, 1)$, and that is the case for the symptomatic populace for $\tau \in (0.95, 1)$.

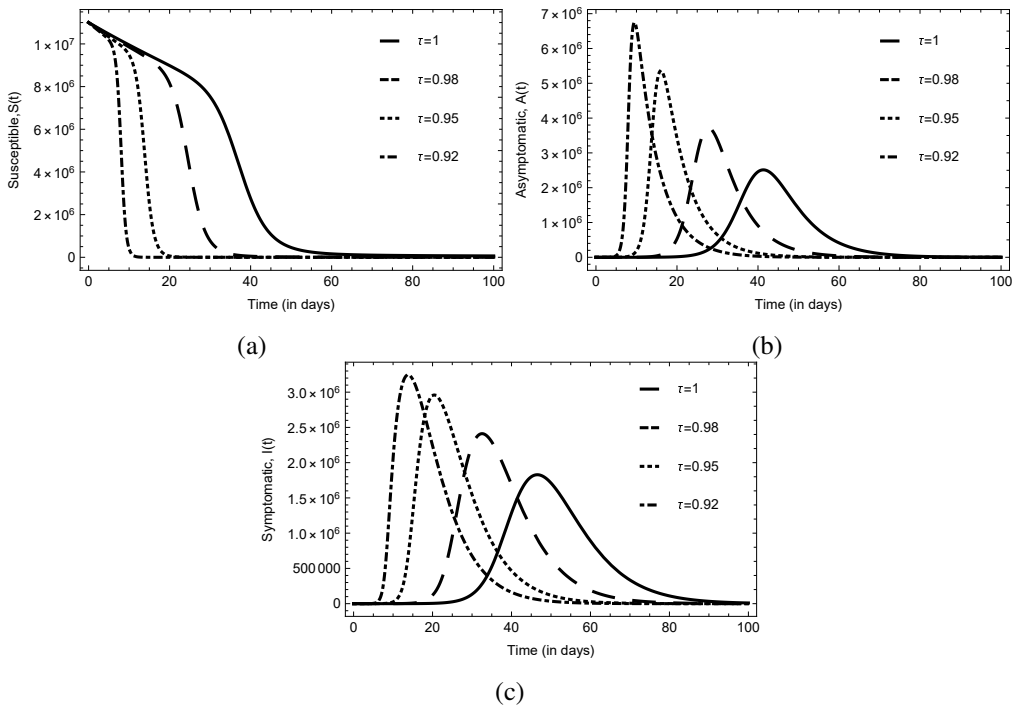

Figure 2. Time series plots of the state variables of the proposed CoVID-19 model with various differential orders τ, and the rest of the parameters are taken from Table 1.

In Figure 3, we give the relationship between the asymptomatic infected people and the symptomatic infected individuals for two different values of $\tau = 1, 0.95$ by keeping $\xi = 1.25$. We see that the behaviour of asymptomatics and symptomatics are periodic in nature. This results in instability of the co-existing equilibrium point of the model. It can be controlled by bringing restriction to the rate η. Even the death rate d may also have significant role in the optimization of $\mathcal{R}_0$. To verify the plot, we present Figure 4, representing the graph of $\mathcal{R}_0$ within a limit of $\eta \in [0, 0.2]$ with three different values of d. It is observed that $\mathcal{R}_0$ can be decreased for very small death rate, irrespective of the CoVID-19 symptom detection.

In Figure 5 we provide the effects of transition rate η on (a) asymptomatic individual, and (b) symptomatic individuals for four different values of $\eta = 0.01, 0.015, 0.1, 0.15$. The graphs are plotted using Wolfram Mathematica. From the achieved figures, we can say that the given model immensely depends on the differential order and indicates more degree of malleability. In addition to that, the

fractional method provides more fascinating results than the integer order model and allows to better testing the results thus obtained. The graphical simulations between $\tau = 1$ and $\tau = 0.95$ are more precise to compare with the real data. The state variables are exhibiting acceptable natures between these two values of τ. The parameter ξ plays a very vital role in the simulations. More diversities in the graphical simulations can be seen at the different values of ξ.

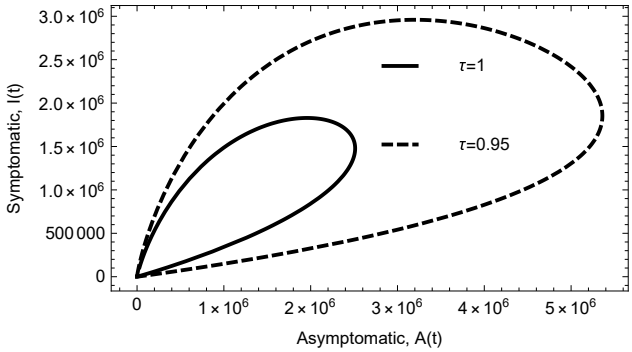

Figure 3. Parametric plot of Symptomatic vs; asymptomatic population for integer model ($\tau = 1$) and fractional model ($\tau = 0.95$), and the rest of the parameters' values are from Table 1.

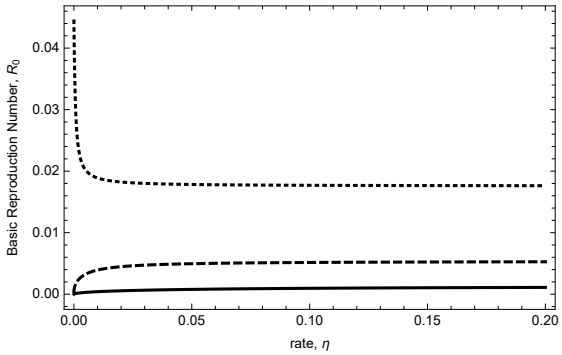

Figure 4. Plot of $\mathcal{R}_0$ w.r.t. rate η by varying $d = 0.1$ (bold), 0.01 (dashed), 0.001 (dotted), and the rest of the parameters' values are from Table 1.

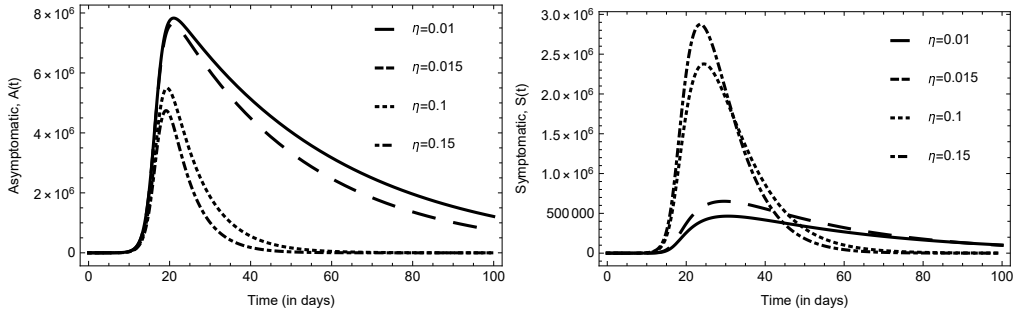

(a) (b)

Figure 5. Time series plots of Asymptomatic and Symptomatic populaces with varying η, and the rest of the parameters' values are from Table 1.

9. Conclusions

In the last 25 to 30 years, numerous deadly viral infections have caused damage in various parts around the globe. Here, we have focused on the time-integer and time-fractional CoVID-19 model with memory effect. The numerical simulation is done with the Ms-DTM and the PC scheme for the new generalized Caputo-type fractional derivative. The sensitivity analysis of $\mathcal{R}_0$ has given a clear picture of the most crucial parameter to tackle. The stability analysis of the PC scheme is done using important lemmas. The qualitative analysis of both systems, integer and fractional, is also done by fixed point theorems. The results help to provide ideas of CoVID-19 cases where asymptomatic cases are rising. The nature of the achieved solutions has been analyzed with the help of graphs, and we have also provided the importance and effects of both the integer order and fractional order systems. We have taken a non-uniform mesh for numerical calculations, and the parameter ξ helped to study the model more precisely in comparison to the real data, which is one of the important characteristics of the PC scheme. For the solution of this pandemic model, we showed various graphical results at the different values of τ. The present study epitomizes the applications of the PC scheme and chose fractional operator while surveying real world problems. For the contemplated system of equations instantiating the infection model, the solution is settled with the help of the NGCFD.

Acknowledgments

The authors extend their appreciation to the Deputyship for Research & Innovation, Ministry of Education, Saudi Arabia for funding this research work through the Project Number QU-IF-2-2-2-26355. The authors also thank to Qassim University for technical support.

Conflict of interest

The authors declare no conflicts of interest.

References

1. A. Ali, F. Alshammari, S. Islam, M. Khan, S. Ullah, Modeling and analysis of the dynamics of novel coronavirus (COVID-19) with Caputo fractional derivative, *Results Phys.*, **20** (2021), 103669. http://dx.doi.org/10.1016/j.rinp.2020.103669
2. S. Akindeinde, E. Okyere, A. Adewumi, R. Lebelo, O. Fabelurin, S. Moore, Caputo fractional-order SEIRP model for COVID-19 epidemic, *Alex. Eng. J.*, **61** (2022), 829–845. http://dx.doi.org/10.1016/j.aej.2021.04.097
3. I. Ahmed, G. Modu, A. Yusuf, P. Kumam, I. Yusuf, A mathematical model of Coronavirus disease (COVID-19) containing asymptomatic and symptomatic classes, *Results Phys.*, **21** (2021), 103776. http://dx.doi.org/10.1016/j.rinp.2020.103776
4. A. Anirudh, Mathematical modeling and the transmission dynamics in predicting the Covid-19-what next in combating the pandemic, *Infectious Disease Modelling*, **5** (2020), 366–374. http://dx.doi.org/10.1016/j.idm.2020.06.002

5. L. Barros, M. Lopes, F. Pedro, E. Esmi, J. Santos, D. Sánchez, The memory effect on fractional calculus: an application in the spread of COVID-19, *Comp. Appl. Math.*, **40** (2021), 72. http://dx.doi.org/10.1007/s40314-021-01456-z
6. S. Biswas, J. Ghosh, S. Sarkar, U. Ghosh, COVID-19 pandemic in India: a mathematical model study, *Nonlinear Dyn.*, **102** (2020), 537–553. http://dx.doi.org/10.1007/s11071-020-05958-z
7. M. Caputo, M. Fabrizio, On the notion of fractional derivative and applications to the hysteresis phenomena, *Meccanica*, **52** (2017), 3043–3052. http://dx.doi.org/10.1007/s11012-017-0652-y
8. B. Dhar, P. Gupta, A numerical approach of tumor-immune model with B cells and monoclonal antibody drug by multi-step differential transformation method, *Math. Method. Appl. Sci.*, **44** (2021), 4058–4070. http://dx.doi.org/10.1002/mma.7009
9. B. Dhar, P. Gupta, M. Sajid, Solution of a dynamical memory effect COVID-19 infection system with leaky vaccination efficacy by non-singular kernel fractional derivatives, *Math. Biosci. Eng.*, **19** (2022), 4341–4367. http://dx.doi.org/10.3934/mbe.2022201
10. V. Erturk, P. Kumar, Solution of a COVID-19 model via new generalized Caputo-type fractional derivatives, *Chaos Soliton. Fract.*, **139** (2020), 110280. http://dx.doi.org/10.1016/j.chaos.2020.110280
11. Y. Feng, X. Yang, J. Liu, On overall behavior of Maxwell mechanical model by the combined Caputo fractional derivative, *Chinese J. Phys.*, **66** (2020), 269–276. http://dx.doi.org/10.1016/j.cjph.2020.05.006
12. M. Islam, A. Peace, D. Medina, T. Oraby, Integer versus fractional order SEIR deterministic and stochastic models of measles, *Int. J. Environ. Res. Public Health*, **17** (2020), 2014. http://dx.doi.org/10.3390/ijerph17062014
13. A. Jajarmi, D. Baleanu, A new fractional analysis on the interaction of HIV with CD4+ T-cells, *Chaos Soliton. Fract.*, **113** (2018), 221–229. http://dx.doi.org/10.1016/j.chaos.2018.06.009
14. U. Katugampola, Existence and uniqueness results for a class of generalized fractional differential equations, arXiv:1411.5229.
15. E. Kharazmi, M. Cai, X. Zheng, Z. Zhang, G. Lin, G. Karniadakis, Identifiability and predictability of integer-and fractional-order epidemiological models using physics-informed neural networks, *Nat. Comput. Sci.*, **1** (2021), 744–753. http://dx.doi.org/10.1038/s43588-021-00158-0
16. K. Kozioł, R. Stanisławski, G. Bialic, Fractional-order sir epidemic model for transmission prediction of covid-19 disease, *Appl. Sci.*, **10** (2020), 8316. http://dx.doi.org/10.3390/app10238316
17. C. Li, Y. Zhu, C. Qi, L. Liu, D. Zhang, X. Wang, et al., Epidemic dynamics of COVID-19 based on SEAIUHR model considering asymptomatic cases in Henan province, China, *Research Square*, in press. http://dx.doi.org/10.21203/rs.3.rs-50050/v1
18. C. Li, F. Zeng, The finite difference methods for fractional ordinary differential equations, *Numer. Funct. Anal. Opt.*, **34** (2013), 149–179. http://dx.doi.org/10.1080/01630563.2012.706673
19. D. McNamara, About 80% of asymptomatic people with CoVID-19 develop symptom, *Medscape Medical News*, September 28, 2020.

20. P. Naik, K. Owolabi, J. Zu, M. Naik, Modeling the transmission dynamics of COVID-19 pandemic in Caputo type fractional derivative, *J. Multiscale Model.*, **12** (2021), 2150006. http://dx.doi.org/10.1142/S1756973721500062

21. P. Naik, J. Zu, M. Ghori, M. Naik, Modeling the effects of the contaminated environments on COVID-19 transmission in India, *Results Phys.*, **29** (2021), 104774. http://dx.doi.org/10.1016/j.rinp.2021.104774

22. Z. Odibat, D. Baleanu, Numerical simulation of initial value problems with generalized Caputo-type fractional derivatives, *Appl. Numer. Math.*, **156** (2020), 94–105. http://dx.doi.org/10.1016/j.apnum.2020.04.015

23. Z. Odibat, C. Bertelle, M. Aziz-Alaouni, G. Duchamp, A multi-step differential transform method and application to non-chaotic or chaotic systems, *Comput. Math. Appl.*, **59** (2010), 1462–1472. http://dx.doi.org/10.1016/j.camwa.2009.11.005

24. O. Postavaru, S. Anton, A. Toma, COVID-19 pandemic and chaos theory, *Math. Comput. Simulat.*, **181** (2021), 138–149. http://dx.doi.org/10.1016/j.matcom.2020.09.029

25. I. Podlubny, *Fractional differential equations: an introduction to fractional derivatives, fractional differential equations, to methods of their solution and some of their applications*, Amsterdam: Elsevier, 1999. http://dx.doi.org/10.1016/s0076-5392(99)x8001-5

26. S. Rosa, D. Torres, Parameter estimation, sensitivity analysis and optimal control of a periodic epidemic model with application to HRSV in Florida, *Stat. Optim. Inf. Comput.*, **6** (2018), 139–149. http://dx.doi.org/10.19139/soic.v6i1.472

27. P. van den Driessche, J. Watmough, Reproduction numbers and sub-threshold endemic equilibria for compartmental models of disease transmission, *Math. Biosci.*, **180** (2002), 29–48. http://dx.doi.org/10.1016/S0025-5564(02)00108-6

28. S. Yadav, D. Kumar, J. Singh, D. Baleanu, Analysis and dynamics of fractional order Covid-19 model with memory effect, *Results Phys.*, **24** (2021), 104017. http://dx.doi.org/10.1016/j.rinp.2021.104017

29. M. Zamir, G. Zaman, A. Alshomrani, Sensitivity analysis and optimal control of anthroponotic cutaneous leishmania, *PloS One*, **11** (2016), 0160513. http://dx.doi.org/10.1371/journal.pone.0160513

AIMS Press